AI Engineering
https://www.sciltp.com/journals/aieng

Article

An LSTM-Driven Efficient Solution Algorithm of Economic Dispatch with Integral Constraints for Energy-Intensive Enterprise Microgrids

Yuqian Ying, Qiaozhu Zhai, Yuzhou Zhou * and Jiexing Zhao

Systems Engineering Institute, MOEKLINNS, Xi'an Jiaotong University, Xi'an 710049, China
* Correspondence: yzzhou@sei.xjtu.edu.cn

How To Cite: Ying, Y.; Zhai, Q.; Zhou, Y.; et al. An LSTM-Driven Efficient Solution Algorithm of Economic Dispatch with Integral Constraints for Energy-Intensive Enterprise Microgrids. *AI Engineering* **2025**, *1*(1), 5. https://doi.org/10.53941/aieng.2025.100005

Received: 21 July 2025
Revised: 26 August 2025
Accepted: 1 September 2025
Published: 5 September 2025

Abstract: Accurate and efficient economic dispatch (ED) is important for the operation of energy-intensive microgrids. The traditional discrete modeling method cannot meet the actual needs of enterprises. The exact representation of device-specific operational dynamics requires the solution of continuous-time differential equations to determine their respective performance curves, which is generally computationally intractable. Motivated by these challenges, this paper proposes a data-driven efficient solution algorithm of ED with integral constraints. Specifically, first, to better capture the real-time characteristics of power generation, this paper formulates an energy-balanced-constrained ED model by introducing integral constraints into the dispatch formulation. Second, a pair of boundary constraints is applied to reformulate the continuous-time integral constraints into quadratic equations. Then, a data-driven efficient solution algorithm is developed, which requires only an initial point satisfying all inequality constraints. To enhance the quality of the initial point, a long-short-term memory (LSTM) neural network is trained to predict the warm-start point. The numerical results implemented in an energy-intensive microgrid system validate the feasibility and optimality of the proposed method.

Keywords: economic dispatch; energy-intensive microgrid; integral constraints; data-driven; LSTM

1. Introduction

For energy-intensive industries such as iron and steel enterprises, electricity expenditure can constitute up to 20% of their total operational costs [1–3]. While ensuring production-related objectives are met, minimizing electricity costs becomes a critical goal. Therefore, compared with other microgrid systems, energy-intensive enterprise microgrids require more sophisticated power dispatch modeling.

The Economic Dispatch (ED) problem in power systems refers to optimizing the generation schedules of units so that the system's load demand and operational constraints are satisfied at a minimum cost, which includes generation cost, fuel cost, start-up cost, and other related costs [4, 5]. By determining the optimal generation schedule without altering the generation process or hardware, ED offers a practical solution for reducing energy consumption and emissions. In the context of escalating energy and environmental concerns, such optimization is essential for promoting the sustainable development of energy-intensive industries.

Typically, conventional ED problems have been formulated using discrete-time models, where the time horizon is divided into several periods, and the average power output of each generating unit at each time period is treated as a decision variable. For example, a discrete-time coordinated dispatch framework between the power system and energy-intensive enterprises under intrinsic time of use (TOU) prices was designed in Ref. [6], which requires only several pieces of boundary information for interaction. Hou et al. proposed a data-driven discrete-time two-stage dispatch model for microgrids with consideration of multiple demand responses [7]. Besides, a discrete-time convex

hull model for the self-scheduling model was proposed in [8] for energy-intensive enterprises. And Zhao et al. proposed a low-carbon dispatching methodology for power systems to address energy-intensive load regulation [9].

In terms of solving, these formulations typically lead to an integer programming (IP) or mixed-integer programming (MIP) problem [4, 10]. Based on such models, various optimization methods have been employed to solve the ED problem, including interior point methods [10, 11], quadratic programming [12], and Lagrangian relaxation approaches [13–15]. However, due to the instantaneous characteristic of power generation, discrete-time models often fail to accurately capture the real-time operation of power systems, which may result in unrealistic scheduling plans, e.g., ramping jumps of units [16].

To achieve more precise scheduling, in Ref. [16], integral constraints are introduced to more precisely describe the relationship among energy output, power generation and ramping rates, and the traditional power balance constraint is reformulated into an energy balance form. By mathematical derivation, the continuous-time model can be further transformed into an equivalent nonlinear programming (NLP) problem [16]. Based on this foundation, in Ref. [17], the continuous-time framework with integral constraints is applied to the unit commitment (UC) problem and a novel power-based staircase transmission-constrained UC formulation is proposed, which effectively captures the implicit coupling between ramping constraints and spinning reserve requirements. Moreover, a Lagrangian relaxation-based algorithm is designed to obtain the optimal solution in [17]. In Ref. [18], the framework is extended to a microgrid by incorporating both integral constraints and nonanticipativity, and a three-stage numerical solution method is proposed to derive an optimal dispatch strategy.

Additionally, data-driven techniques based on artificial neural network (ANN) have been increasingly employed in power systems [5, 19]. At present, most ANN forecasting models are utilized to predict load [20], renewable generation [21], and market electricity price [22], serving as decision-support tools. In Ref. [23], an ANN-based framework is proposed to enable fast economic dispatch in an integrated electricity-gas system by learning from simulation data generated via a piecewise-linear model-driven approach, where the neural network directly maps system load profiles to optimal scheduling outcomes.

For the equivalent NLP problem in [16], which simplifies integral constraints to convex constraints, the current Gurobi solver is incapable of solving it directly and can only provide approximate solutions through linearization. The sequential quadratic programming method in [16] and the Lagrangian relaxation-based method in [17] both fail to yield a feasible solution if the iteration is terminated prematurely, i.e., before convergence to the optimal point. The three-stage solution method in [18] requires an initial feasible solution in the first stage to start the iteration. However, under the strict equality constraint of energy balance, identifying such a feasible starting point is non-trivial.

In this paper, we formulate a continuous-time model for the ED problem in energy-intensive microgrids, and propose a data-driven efficient solution algorithm with initial point forecasting. The main contributions are summarized as follows:

1. An energy-balance-constrained formulation of the ED problem with integral constraints in energy-intensive microgrids is proposed to achieve more sophisticated power dispatching and energy saving.
2. A model transformation is employed to reformulate the continuous-time integral constraints into quadratic equations. And then, an efficient solution method is designed, which only requires an initial point that satisfies all the inequality constraints.
3. An LSTM-based forecasting model is developed to obtain good warm-start points for the proposed method to accelerate the entire solving process.

The rest of this paper is organized as follows. Section 2 presents the continuous-time ED formulation and its transformation to an NLP problem. Section 3 details the proposed solution algorithm and LSTM warm-start point forecasting mechanism. Case studies on an energy-intensive microgrid system with 8 units and 24 hours are discussed in Section 4, followed by conclusions in Section 5.

2. Problem Formulation

2.1. Energy-Balance-Constrained ED Formulation

Consider an energy-intensive microgrid with I units and suppose the schedule is divided into K time periods. The proposed continuous-time energy-balance-constrained ED formulations maintain a similar structure to conventional discrete-time ED formulations.

Objective:

$$\min_{p_i(t),e_i(k)} J = \sum_{i=1}^{I}\sum_{k=1}^{K} C_i(e_i(k)) \tag{1}$$

Equation (1) means total electricity cost should be minimized and quadratic generation cost function is adopted in many practical applications [24], where

$$C_i(e_i(k)) = a_i\big(e_i(k)\big)^2 + b_i e_i(k) + c_i \tag{2}$$

Constraints:

- Energy balance constraints

$$\sum_{i=1}^{I} e_i(k) = D(k),\ k = 1, 2, \ldots, K \tag{3}$$

- Power output limit constraints

$$\underline{p}_i \le p_i(t) \le \overline{p}_i, \forall t \in [0, K\tau] \tag{4}$$

- Ramp rate limit constraints

$$-\Delta_i \le u_i(t) \le \Delta_i, \forall t \in [0, K\tau] \tag{5}$$

- Integral constraints

$$e_i(k) = \int_{(k-1)\tau}^{k\tau} p_i(t)\, dt \tag{6}$$

$$p_i(t) = p_i(0) + \int_0^t u_i(\xi)\, d\xi, \quad \forall t \in [0, K\tau] \tag{7}$$

- Initial constraints

$$p_i(0) = p_{i,0}^* \tag{8}$$

Equation (3) ensures the total energy production equals the load requirements. Equations (4) and (5) represent the upper and lower bounds on the power output and ramp rate of units during operation. Equations (6) and (7) show the integral relationships between the power production and the power output, and between power output and ramp rate, respectively. These two constraints are the core formulation that distinguishes the continuous-time model from the discrete-time model. Equation (8) is the initial condition of the power output of units where $g_{i,0}^*$ is given.

2.2. Model Transformation

It is seen that with both discrete and continuous constraints, the energy-balanced-constrained ED model (1)–(8) is difficult to solve directly. However, according to the derivation in Ref. [16], this original problem could be transformed into an equivalent NLP problem form:

$$\min_{p_{i,k}, e_i(k)} \sum_{i=1}^{I}\sum_{k=1}^{K} a_i\big(e_i(k)\big)^2 + b_i e_i(k) + c_i \tag{9a}$$

$$\text{s.t.} \quad \sum_{i=1}^{I} e_i(k) = D(k),\ k = 1, 2, \ldots, K \tag{9b}$$

$$|p_{i,k} - p_{i,k-1}| \le \Delta_i \tau \tag{9c}$$

$$\underline{p}_i \le p_{i,k} \le \overline{p}_i \tag{9d}$$

$$\underline{e}_i(p_{i,k-1}, p_{i,k}) \le e_i(k) \le \overline{e}_i(p_{i,k-1}, e_{i,k}) \tag{9e}$$

$$p_{i,0} = p_{i,0}^* \tag{9f}$$

The upper and lower bound of $e_i(k)$ in Equation (9e) are expressed as binary functions of $p_{i,k-1}$ and $p_{i,k}$:

$$\overline{e}_i(p_{i,k-1}, p_{i,k}) = \begin{cases} -\dfrac{(p_{i,k-1} - \bar{p}_i)^2 + (p_{i,k} - \bar{p}_i)^2}{2\Delta_i} + \bar{p}_i\tau, \\ \text{if } p_{i,k-1} + p_{i,k} \ge 2\bar{p}_i - \Delta_i\tau \\ -\dfrac{(p_{i,k-1} - p_{i,k})^2}{4\Delta_i} + \dfrac{\tau}{2}(p_{i,k-1} + p_{i,k}) + \dfrac{\Delta_i}{4}\tau^2, \\ \text{if } p_{i,k-1} + p_{i,k} < 2\bar{p}_i - \Delta_i\tau \end{cases} \tag{10}$$

$$\underline{e}_i(p_{i,k-1}, p_{i,k}) = \begin{cases} \dfrac{(p_{i,k-1}-\underline{p}_i)^2 + (p_{i,k}-\underline{p}_i)^2}{2\Delta_i} + \underline{p}_i\tau; \\ \text{if } p_{i,k-1} + p_{i,k} < 2\underline{p}_i + \Delta_i\tau \\ \dfrac{(p_{i,k-1}-p_{i,k})^2}{4\Delta_i} + \dfrac{\tau}{2}(p_{i,k-1}+p_{i,k}) - \dfrac{\Delta_i}{4}\tau^2; \\ \text{if } p_{i,k-1} + p_{i,k} \geq 2\underline{p}_i + \Delta_i\tau \end{cases} \tag{11}$$

Since the objective function (9a) is quadratic, all constraints except (9e) are linear, and the piecewise quadratic Equations in (10) and (11) are smooth convex/concave functions (with detailed proof provided in Ref. [16]) which demonstrates that constraint (9e) is convex, the problem (9) can be further reformulated as a convex programming problem. To simplify the formulation, the equivalent convex programming problem is further transformed into the following standard NLP form:

$$\min_{X,Y} \quad f(X,Y) = Y^{\mathrm{T}}AY + B^{\mathrm{T}}Y + C \tag{12a}$$

$$\text{s.t.} \quad G_i(X,Y) \leq 0, \quad i = 1,2,\ldots,6IK \tag{12b}$$

$$H_j(X,Y) = 0, \quad j = 1,2,\ldots,K \tag{12c}$$

where X is the vector of $p_{i,k}$, Y is the vector of $e_i(k)$. A is the quadratic coefficient matrix of fuel cost function (2) , while B and C are the linear, constant vector, respectively. The inequality constraints (9c)–(9e) are listed in Equation (12b) and the equality constraints (9b) are rewritten as Equation (12c).

3. Solution Method

It is easy to see that for the problem(14), solutions satisfying the inequality constraints (12b) can be readily obtained, while the main difficulty lies in the equality constraint (12c). Therefore, the core idea of the proposed method is to start from an initial interior point that satisfies the inequality constraints, and to perform an iterative search within the feasible region defined by inequalities to quickly obtain a good feasible, or even optimal, solution. The algorithm framework can be summarized in Figure 1. Specifically, the procedure begins with initializing the system parameters and generating an interior point that meets all inequality constraints. Then, active inequality constraints and unsatisfied equality constraints are filtered, based on which an linear programming (LP) subproblem is solved to obtain the search direction. The maximum feasible step length and the optimal search step are computed to update the current point. These steps are repeated iteratively until the termination criterion is satisfied, i.e., the error of each energy balance equality constraint and the difference in cost between two consecutive iterations are both less than prescribed thresholds. Finally, the algorithm outputs the generation power and energy at convergence.

To implement the proposed algorithm, it is essential to specify how to construct the search direction, select the step size at each iteration, and obtain a proper initial point.

3.1. Search Direction Construction

There are two fundamental principles guiding the determination of the search direction at each iteration: (1) simultaneously reduce the objective function and approach satisfaction of the energy balance constraint as much as possible; (2) remain within the feasible region defined by the inequality constraints.

In accordance with Principle(1), the energy balance constraint is incorporated into the objective function (12a) as a penalty term, and the reformulated optimization problem can be expressed as:

$$\min_{X,Y} \quad F(X,Y) = f(X,Y) + \lambda\|EY - D\|_2^2 \tag{13a}$$

$$\text{s.t.} \quad G_i(X,Y) \leq 0, \quad i = 1,2,\ldots,6IK \tag{13b}$$

where λ is the penalty factor, increasing as the iteration proceeds to enforce the satisfaction of the energy balance constraint (3). E is the coefficient matrix of constraint (3), and D is the corresponding right-hand-side vector.

Considering Principle(1), the angle between the gradient of the reformulated objective (13a) and the search direction should be minimized. Principle(2) implies that when the current point reaches the boundary of the inequality constraints, the subsequent search direction should form an obtuse angle with the gradients of these active inequality constraints. Based on this, the feasible descent direction d can be obtained by solving the following LP

problem:

$$\min_{d} \ \nabla F(X,Y)\cdot d \tag{14a}$$

$$\text{s.t.} \quad \nabla G_{\text{cri},j}(X,Y)\cdot d \le 0, \quad j \in I(X,Y) \tag{14b}$$

$$-1 \le d_i \le 1, \quad i = 1,2,\ldots,2IK \tag{14c}$$

where $I(X,Y)$ is the active inequality constraints set at the current point. It should be noted that, in order to quantify the angle between d and $\nabla F(X,Y)$, d is expected to have unit length, i.e., $\|d\|_2 = 1$. However, for simplification, we treat it as a linear constraint in (14c), which means for each nonzero component (positive/negative) of $\nabla F(X,Y)$, the corresponding d_i should be as close to -1 or $+1$ as possible to minimize $\nabla F(X,Y)\cdot d$.

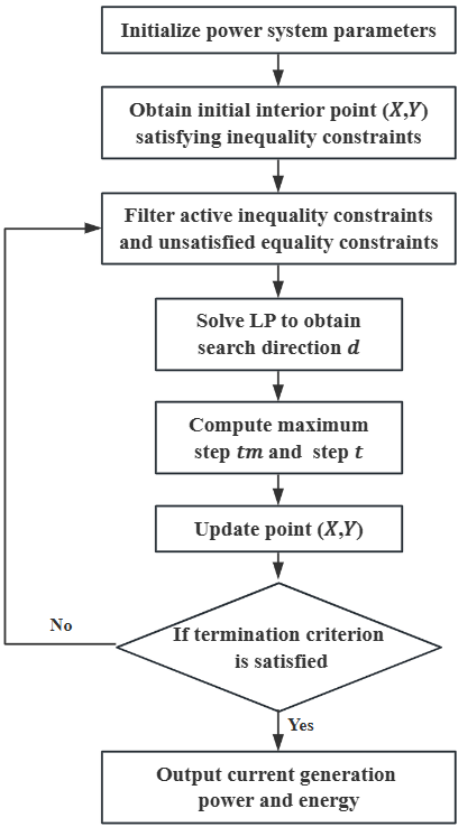

Figure 1. Algorithm framework chart.

3.2. Step Size Selection

After obtaining the search direction d by solving problem(15), the step size of the current iteration can be determined by a 1D line search method:

$$\min_{t} \ \varphi(t) = F(X + t\,d_X,\, Y + t\,d_Y) \tag{15a}$$

$$\text{s.t.} \quad 0 \le t \le t_{\text{m}} \tag{15b}$$

Similarly, there are two requirements for the search step size: (1) the updated point after the iteration must satisfy all the inequality constraints; (2) the distance between the updated point and the energy balance constraint should not increase. Accordingly, a system of equations can be formulated to compute the maximum allowable step size t_{m}. Requirement (1) includes $4IK$ linear equations and $2IK$ nonlinear equations which are derived from constraints (9e). Requirement (2) can be expressed as:

$$\|E(Y + td_Y) - D\|_2 \le \|EY - D\|_2 \tag{16}$$

Further expanding and simplifying yields:

$$(Ed_Y)^{\text{T}}(Ed_Y)t_{\text{m}} = -2(EY - D)^{\text{T}}(Ed_Y) \tag{17}$$

Since Equation (17) is also a linear equation, the computational cost of calculating t_{m} mainly lies in solving the nonlinear equations. The maximum step size calculation algorithm is tabulated in Algorithm 1: Given current point (X, Y) and search direction d, we first solve all linear equations to obtain an initial t; then judge whether t satisfies all convex constraints, if it does, accept $t_{\mathrm{m}} = t$, otherwise use a binary search to find t_{m}, thereby avoiding direct solution of nonlinear equations. The bool variable is_eq_tm2 is used to determine whether t_{m} corresponds exactly to the solution of Requirement (2). If true, take $t = t_{\mathrm{m}}/2$ to avoid oscillation near the energy balance constraint.

Algorithm 1 Maximum Step Size Calculation

Input: (X, Y), d, system parameters
Output: t_{m}, is_eq_tm2

1: Linear inequality constraints:
tm1_list $\leftarrow \left\{-\text{Bound}/d \;\middle|\; \text{valid and positive}\right\}$
if non-empty **then** $t_1 \leftarrow \min(\text{tm1\_list})$, **else** $t_1 \leftarrow 10^{20}$
2: Energy balance constraint:
$M \leftarrow E \cdot d_Y$, $a \leftarrow M^\top M$, $b \leftarrow 2(EY - D)^\top M$
if $a \neq 0$ and $b < 0$ **then** $t_2 \leftarrow -b/a$, **else** $t_2 \leftarrow 10^{20}$
3: Convex inequality constraints:
Initialize $temp \leftarrow \min[t_1, t_3]$
if all convex constraints satisfied **then** $t_{\mathrm{m}} = temp$
else binary search:
$left \leftarrow 0, right \leftarrow temp$
while $|right - left| > 10^{-6}$:
$temp \leftarrow (\text{left} + \text{right})/2$
if convex constraint violated **then** $right \leftarrow temp$
else $left \leftarrow temp$
$t_{\mathrm{m}} = temp$
4: Final check:
if $|t - t_2| < 10^{-6}$ **then** is_eq_tm3 $\leftarrow$ True
else is_eq_tm2 $\leftarrow$ False
5: **return** t_{m}, is_eq_tm2

3.3. Initial Point Forecasting

By utilizing data obtained from solving the piecewise linear approximation of the original problem (12) under different load demands using Gurobi, a forecasting model can be constructed to provide a good warm-start point for the above algorithm. In a power system scheduling problem with I units and K time periods, the model needs to handle long time-series sequence-to-sequence (Seq2Seq) prediction. To this end, a Seq2Seq forecasting model with LSTM is adopted in this paper. The overall framework is illustrated in Figure 2, and the detailed configuration is shown in Table 1.

Since the physical parameters of units are generally time-invariant, they are first processed by a multilayer perceptron (MLP) to form an $8I$-dimensional static embedding, where each unit is represented by 1 index and 7 physical parameters. This embedding is concatenated with the dynamic load at the k-th time period, $D(k)$, to form the input vector for each time step, resulting in an $(8I + 1)$-dimensional input feature. Then, the input sequences are fed into 2 stacked LSTM layers, each with 128 hidden nodes, which capture the temporal dependencies by transferring hidden state (h_k) and cell state (c_k) to the next time step. Finally, the forecasting model output is passed through a fully connected (FC) layer to yield an $(I + I)$-dimensional vector, representing the power outputs and energy generations of I units at each time step. The Z-score normalization (StandardScaler) is used to process input data, and it should be noted that considering the significant difference in magnitude between the load data and the static unit parameters, the two types of inputs are normalized separately.

This model effectively captures both static and dynamic features of the system, making it suitable for long-term forecasting. However, it should be noted that purely reinforcement learning or deep learning methods cannot guarantee the satisfaction of power system constraints, and thus post-processing or correction of the predicted results is required.

Table 1. Forecasting Model Configuration.

No.	Item	Descripition
1	LSTM layers	2
2	FC layer	1
3	Hidden Size	128
4	Input feature	$8I + 1$
5	Output	$I + I$
6	Loss function	MSELoss
7	Optimizer	Adam
8	Learning rate	1e-3
9	Normalization	StandardScaler

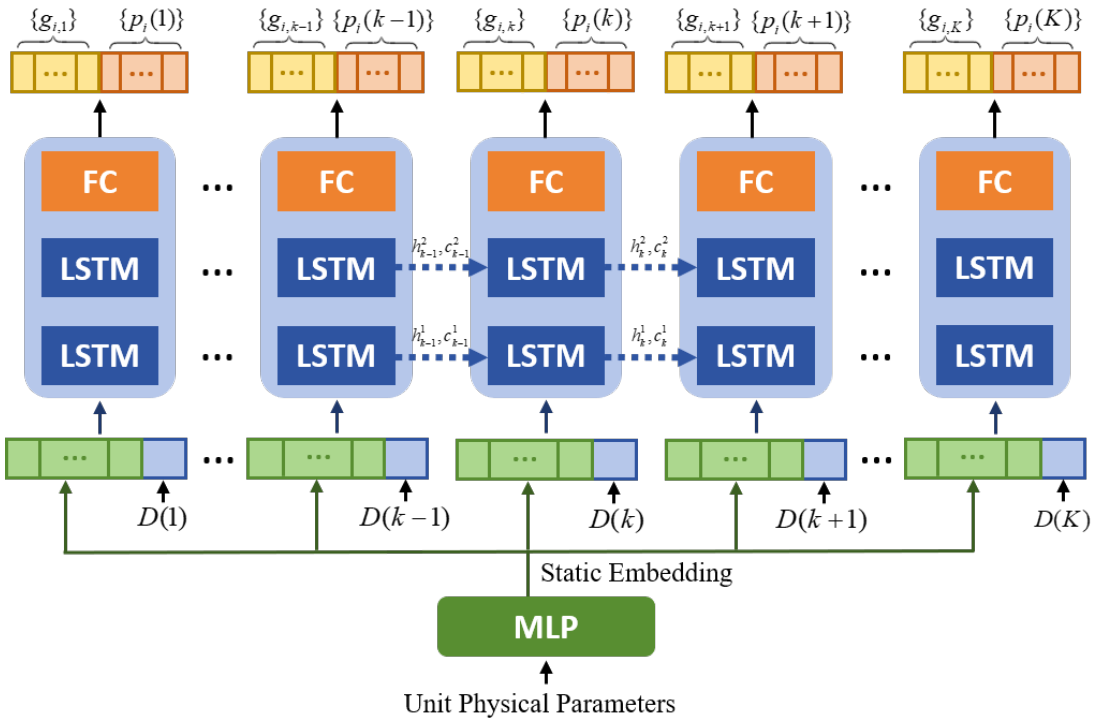

Figure 2. The Framework of the initial point forecasting model.

4. Case Studies

4.1. Basic Information of Test Case

To better evaluate the performance of the proposed algorithm, we conduct numerical testing based on the 24-hour optimal scheduling case of an 8-unit system. This case corresponds to model(1)–(8), which includes $I = 8, K = 24, \tau = 1h$. The detailed unit parameters are shown in Table 2 and system load data is provided in Table 3.

The testing is implemented with Python 3.8.20 on a 3.60 GHz PC with 32.0 GB RAM. The LP problem(16) for search direction is solved using PuLP 2.8.0.

Table 2. Physical Parameters of Units.

Unit i	$\overline{p}_i$ (MW)	$\underline{p}_i$ (MW)	Δ_i (MW/h)	a_i (\$/MWh^2)	b_i (\$/MWh)	c_i (\$)	$p_{i,0}$ (MW)
1	455	150	600.6	0.00031	17.62	970	300
2	455	150	600.6	0.00031	17.62	970	300
3	180	25	247.0	0.00395	19.50	456	60
4	170	25	243.0	0.00395	19.70	450	55
5	162	25	243.0	0.00399	19.80	445	55
6	162	25	240.0	0.00398	19.70	450	60
7	80	25	144.0	0.00712	22.26	370	30
8	65	10	102.3	0.00222	27.27	665	10

Table 3. System Load Demand at Each Time Period.

k	1	2	3	4	5	6	7	8	9	10	11	12
$D(k)$ (MWh)	765	805	875	915	976	1055	1265	1270	1465	1465	1683	1688
k	13	14	15	16	17	18	19	20	21	22	23	24
$D(k)$ (MWh)	1470	1420	1360	1360	1390	1450	1370	1320	1350	1300	840	760

4.2. Training and Validation Process

The dataset is divided into two mutually exclusive subsets with a ratio of 4:1 for training and validating the performance of the initial point forecasting model. Besides, a supervised learning strategy is employed using historical data. The mean squared error (MSE) is employed as the loss function [25], while the mean absolute error (MAE) is additionally reported to evaluate prediction accuracy.

$$MSE = \frac{1}{N}\sum_{i=1}^{N}(\hat{y}_i - y_i)^2 \tag{18}$$

$$MAE = \frac{1}{N}\sum_{i=1}^{N}|\hat{y}_i - y_i| \tag{19}$$

As shown in Figure 3, the training loss decreases steadily and converges after around 40 epochs, while the validation loss flattens earlier and remains stable throughout the training process. This suggests that the model fits the training data well without overfitting, and generalizes reasonably to unseen data. These results demonstrate that the proposed LSTM-based forecasting model is effective in learning the mapping from load demand to optimal power output and energy production under unit static parameters.

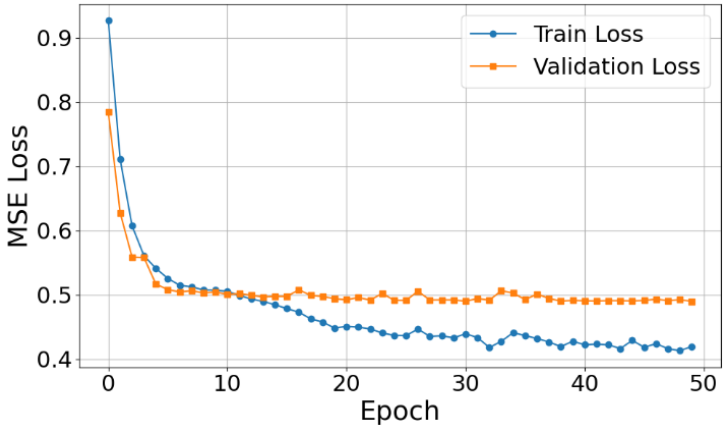

(a) MSE

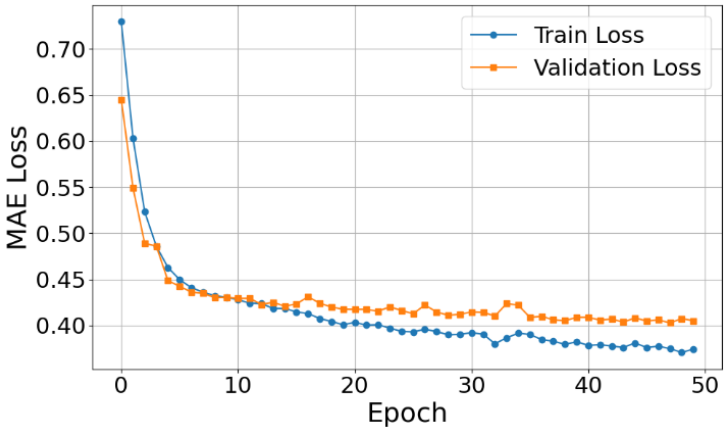

(b) MAE

Figure 3. Loss curves of Training and validation process.

4.3. Testing Results and Analysis

With the above parameters and the initial point predicted by LSTM, the equivalent NLP problem of the power generation system is solved by the proposed algorithm. To quantify the iterative process by which the solution approaches the energy balance constraint, the distance to the energy balance is defined as follows:

$$distance = \|EY - D\|_2 \tag{20}$$

where EY represents the sum of energy production at the current point, and D denotes the load demand.

The convergence performance of the proposed algorithm can be illustrated by tracking the distance to energy balance across iterations. As shown in Figure 4, the algorithm begins with an initial distance of approximately 350, which rapidly decreases within the first 10 iterations, demonstrating strong initial convergence behavior. The distance continues to decline steadily, reaching near-zero values after about 60 iterations, which indicates that the energy balance constraint is effectively satisfied.

Subsequently, the feasibility of the obtained solution is examined. The resulting optimal power generation schedule for each unit over all time periods is shown in Figure 5. The red squares represent the load demand variations. It can be seen that the total power output from all units in each time period satisfies the load demand. In addition, among all the inequality constraints, the upper and lower bounds on energy generation are the least intuitive. Thus, it is necessary to verify whether the generated energy satisfies the boundary constraint (9e) when analyzing the feasibility of the scheduling solution. The energy upper and lower bounds are calculated using Equations (10) and (11), and then compared with the results obtained. Figure 6 presents the energy production and its bounds for Units 2, 4, 6 and 8 for 24-h. As shown in Figure 6, the outputs of units remain within the feasible regions defined by their respective upper and lower bounds.

The optimality of the obtained dispatch solution is further evaluated, based on the cost coefficients a_i, b_i, c_i listed in Table 2. Units 7 and 1, which correspond to the maximum and minimum values of a_i, are selected for comparison. Their power output and system load curves over 24-h are illustrated in Figure 7. As the unit with the lowest generation cost, Unit 1 operates nearly at full capacity during periods of high demand (from 7 h to 22 h). In contrast, Unit 7, which has the highest generation cost, tends to operate at a low output level and only increases its power output when the system demand is really high (from 10h to 13h). Moreover, since the horizontal axis of Figure 7 represents time in hours, it can also be seen that the obtained output curves are relatively smooth, indicating that the ramp rate constraints are well satisfied.

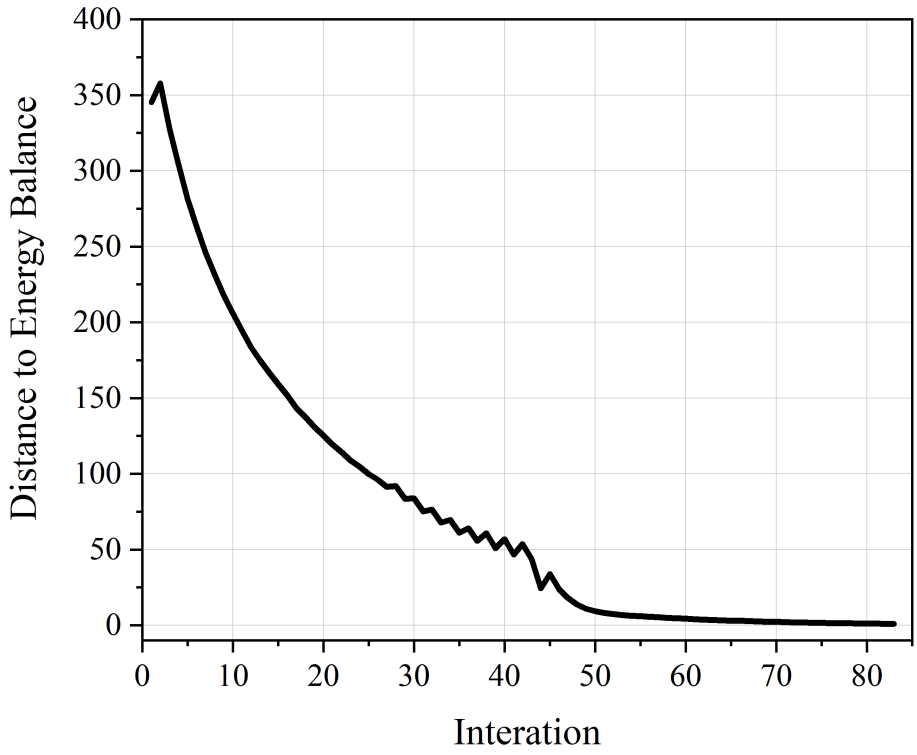

Figure 4. Iterative process of approaching the energy balance.

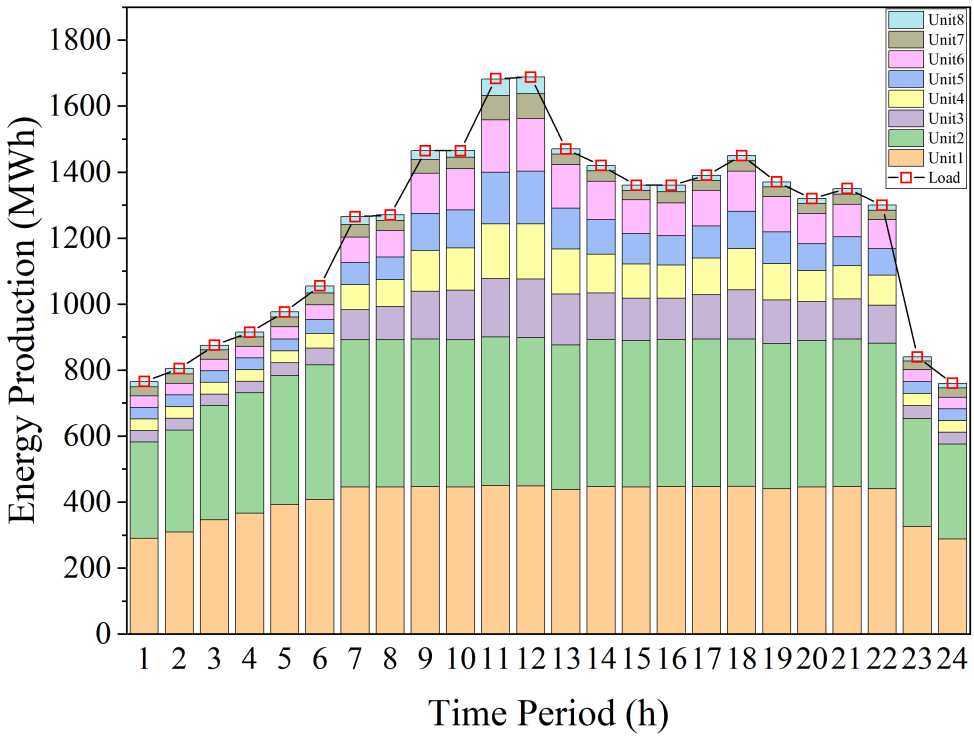

Figure 5. Power dispatch schedules of each unit over all time periods.

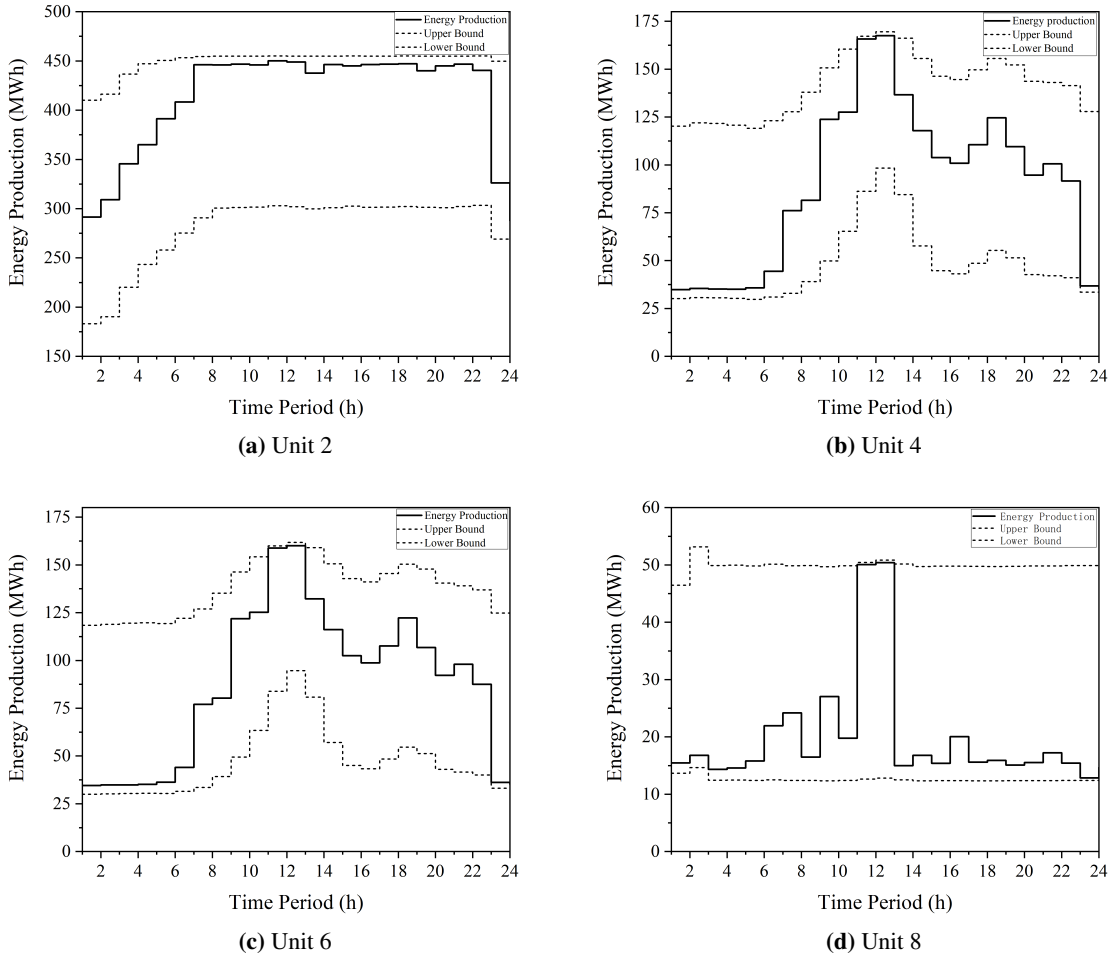

(a) Unit 2 **(b)** Unit 4

(c) Unit 6 **(d)** Unit 8

Figure 6. Energy Production of Units 2, 4, 6, and 8.

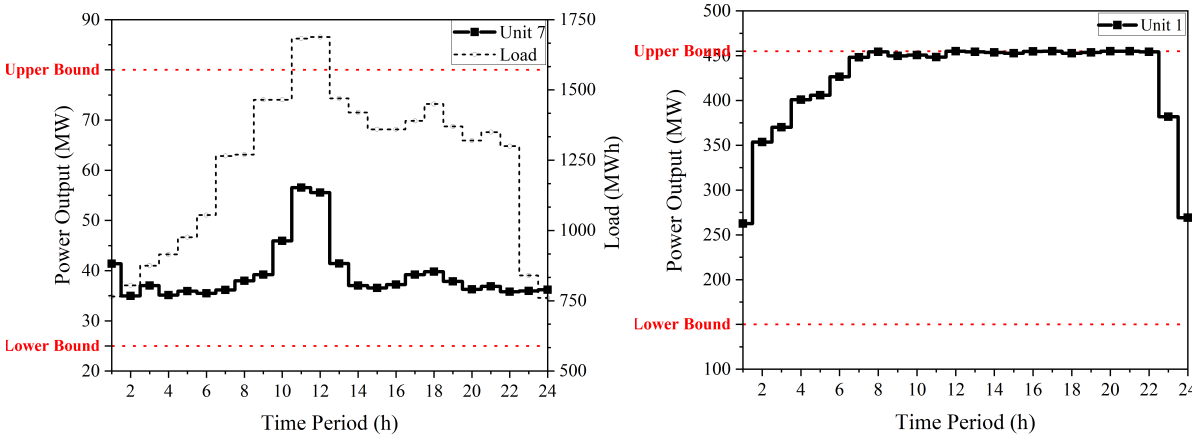

(a) Unit 7 **(b)** Unit 1

Figure 7. Power Output of Units 7, 1 and Load Variation.

5. Conclusions

This paper proposes an energy-balanced-constrained formulation for the ED problem with integral constraints in energy-intensive microgrids. To solve the transformed equivalent NLP problem, a data-driven efficient solution algorithm is designed. The method starts from an initial point that satisfies all inequality constraints and iteratively searches within the feasible region. In addition, an LSTM-based forecasting model is developed to generate high-quality warm start points.

Case studies implemented on an 8-unit system over a 24-h scheduling horizon demonstrate the effectiveness of the proposed approach. The results confirm that the method yields feasible and optimal solutions while maintaining low computational complexity. In the future, we will focus on more general AI-driven technologies to implement the entire algorithm.

Author Contributions

Y.Y.: methodology, software, investigation, validation, visualization, writing—original draft preparation; Q.Z.: conceptualization, methodology, funding acquisition; Y.Z.: methodology, supervision, project administration, writing—reviewing and editing; J.Z.: formal analysis, validation support. All authors have read and agreed to the published version of the manuscript.

Funding

Research supported by Science and Technology Project of State Grid Corporation of China (5400-202255149A-1-1-ZN)).

Institutional Review Board Statement

Not applicable.

Informed Consent Statement

Not applicable.

Data Availability Statement

The test data utilized in this study have been comprehensively presented in the Case Studies section.

Conflicts of Interest

The authors declare no conflict of interest.

Nomenclature

Variables:

$e_i(k)$ Energy production of unit i in time period k (MWh)

$p_i(t)$	Instantaneous power output of unit i at time t (MW)
$p_{i,k}$	Power output of unit i at the end of time period k, that is, $p_{i,k} = p_i(k\tau)$ (MW)
$u_i(t)$	Instantaneous ramp rate of unit i at time t (MW/h)

Parameters:

i	Unit index, $i = 1, 2, \ldots, I$
k	Time period index, $k = 1, 2, \ldots, K$
τ	Length of a time period (h)
$D(k)$	Load demand during time period k (MWh)
$\overline{p}_i$	Upper bound of power outputs of unit i (MW)
$\underline{p}_i$	lower bound of power outputs of unit i (MW)
Δ_i	Ramping rate limit of unit i (MW/h)
$\overline{e}(p_{i,k-1}, p_{i,k})$	Upper bound of energy production of unit i during period k (MWh)
$\underline{e}(p_{i,k-1}, p_{i,k})$	Lower bound of energy production of unit i during period k (MWh)
$C_i(e_i(k))$	Fuel cost function of unit i when energy production is $e_i(k)$ (\$)
a_i, b_i, c_i	Quadratic, linear, constant coefficients of fuel cost function

References

1. Kong, H.; Qi, E.; Li, H.; et al. An MILP model for optimization of byproduct gases in the integrated iron and steel plant. *Appl. Energy* **2010**, *87*, 2156–2163.
2. Liu, K.; Gao, F. Scenario adjustable scheduling model with robust constraints for energy intensive corporate microgrid with wind power. *Renew. Energy* **2017**, *113*, 1–10.
3. Liu, K.; Guan, X.; Gao, F.; et al. Self-balancing robust scheduling with flexible batch loads for energy intensive corporate microgrid. *Appl. Energy* **2015**, *159*, 391–400.
4. Sand, G.; Engell, S. Modeling and solving real-time scheduling problems by stochastic integer programming. *Comput. Chem. Eng.* **2004**, *28*, 1087–1103.
5. Marzbani, F.; Abdelfatah, A. Economic dispatch optimization strategies and problem formulation: A comprehensive review. *Energies* **2024**, *17*, 550.
6. Niu, T.; Li, F.; Fang, S. Enhanced flexibility utilization and coordinated dispatch method of energy-intensive enterprises in power systems under time of use prices. *IET Renew. Power Gener.* **2023**, *17*, 3609–3623.
7. Hou, H.; Wang, Q.; Xiao, Z.; et al. Data-driven economic dispatch for islanded micro-grid considering uncertainty and demand response. *Int. J. Electr. Power Energy Syst.* **2022**, *136*, 107623.
8. Xiao, Y.; Ding, T.; Mu, C.; et al. Convex hull for self-scheduling energy-intensive enterprises with demand response regulations. *IEEE Trans. Power Syst.* **2024**, *40*, 2003–2013.
9. Zhao, X.; Wang, Y.; Liu, C.; et al. Low carbon scheduling method of electric power system considering energy-intensive load regulation of electrofused magnesium and wind powerfluctuation stabilization. *Appl. Energy* **2024**, *357*, 122573.
10. Pan, S.; Jian, J.; Yang, L. A hybrid MILP and IPM approach for dynamic economic dispatch with valve-point effects. *Int. J. Electr. Power Energy Syst.* **2018**, *97*, 290–298.
11. El-Sayed, W.T.; El-Saadany, E.F.; Zeineldin, H.H.; et al. Fast initialization methods for the nonconvex economic dispatch problem. *Energy* **2020**, *201*, 117635.
12. Xu, B.; Zhang, Y.; Liu, J.; et al. Economic dispatch of micro-grid based on sequential quadratic programming—model and formulation. *E3s Web Conf.* **2019**, *136*, 01010.
13. Guan, X.; Guo, S.; Zhai, Q. The conditions for obtaining feasible solutions to security-constrained unit commitment problems. *IEEE Trans. Power Syst.* **2005**, *20*, 1746–1756.
14. Hemamalini, S.; Simon, S.P. Dynamic economic dispatch using Maclaurin series based Lagrangian method. *Energy Convers. Manag.* **2010**, *51*, 2212–2219.
15. Zhan, J.; Wu, Q.; Guo, C.; et al. Fast λ-iteration method for economic dispatch with prohibited operating zones. *IEEE Trans. Power Syst.* **2013**, *29*, 990–991.
16. Guan, X.; Zhai, Q.; Feng, Y.; et al. Optimization based scheduling for a class of production systems with integral constraints. *Sci. China Ser. Technol. Sci.* **2009**, *52*, 3533–3544.
17. Yuan, W.; Zhai, Q. Power-based transmission constrained unit commitment formulation with energy-based reserve. *IET Gener. Transm. Distrib.* **2017**, *11*, 409–418.
18. Zhao, J.; Z.; Zhai, Q.; Miao, H. Energy Balance Based Power Generation Scheduling of Microgrid with Nonanticipativity. In Proceedings of the 2020 39th Chinese Control Conference (CCC), Shenyang, China, 27–29 July 2020; pp. 1530–1535.
19. Ahmed, A.; Khalid, M. A review on the selected applications of forecasting models in renewable power systems. *Renew. Sustain. Energy Rev.* **2019**, *100*, 9–21.

20. Kalakova, A.; Nunna, H.K.; Jamwal, P.K.; et al. A novel genetic algorithm based dynamic economic dispatch with short-term load forecasting. *IEEE Trans. Ind. Appl.* **2021**, *57*, 2972–2982.
21. Quan, H.; Srinivasan, D.; Khosravi, A. Incorporating wind power forecast uncertainties into stochastic unit commitment using neural network-based prediction intervals. *IEEE Trans. Neural Netw. Learn. Syst.* **2014**, *26*, 2123–2135.
22. Lyu, Z.; Wang, Y.; Wang, J.; et al. Short-term electricity price forecasting G-LSTM model and economic dispatch for distribution system. *IOP Conf. Ser. Earth Environ. Sci.* **2020**, *467*, 012186.
23. Liu, H.; Shen, X.; Guo, Q.; et al. A data-driven approach towards fast economic dispatch in electricity–gas coupled systems based on artificial neural network. *Appl. Energy* **2021**, *286*, 116480.
24. Al Farsi, F.; Albadi, M.; Hosseinzadeh, N.; et al. Economic Dispatch in power systems. In Proceedings of the 2015 IEEE 8th GCC Conference & Exhibition, Muscat, Oman, 1–4 February 2015; pp. 1–6.
25. Huang, T.E.; Guo, Q.; Sun, H.; et al. A deep spatial-temporal data-driven approach considering microclimates for power system security assessment. *Appl. Energy* **2019**, *237*, 36–48.